Approaches for Device-free Multi-User Localization with Passive RFID

Benjamin Wagner, Dirk Timmermann
Institute of Applied Microelectronics and Computer Engineering
University of Rostock
Rostock, Germany
firstname.lastname@uni-rostock.de

Abstract—**User localization information is an important data source for ubiquitous assistance in smart environments and other location aware systems. Mostly there is a need for non-invasive, wireless, privacy preserving technologies. Device-free localization approaches (DFL) provide these advantages with no need for user-attached hardware.**

A common goal within the research of DFL technologies is the distinction and tracking of multiple users in an indoor scenario. In our recent work we show that DFL approaches utilizing completely passive RFID transponders can localize one person very precisely.

In this work we show basic approaches and conduct first experiments in an indoor room DFL scenario for proof of concept and validation. We show that it is possible to distinguish between two users with reasonable precision and computation demand.

Keywords-DFL, RFID, Indoor Localization, Smart Environments, Pervasive Computing, Wireless

I. INTRODUCTION

A big challenge in today's ubiquitous smart technology research is the position estimation of users in indoor environments. User Recognition and Intention Recognition are the superimposed steps for generating intelligent assistance. Sensors which are gathering the information need to be invisible and privacy preserving. Therefor much work was done in the field of Device-free localization (DFL) utilizing wireless radio devices which are installed in the room. The user does not need to wear any attached hardware.

In our recent work we introduce an approach for radio based DFL by replacing most of the active radio beacons used in similar situated approaches with completely passive Radio Frequency Identification (RFID) transponders. That combines the advantages of energy efficiency, because the transponders do not need batteries, and very easy deployment. RFID transponders can very easily be placed i.e. under the carpet, on furniture or behind the wallpaper.

Another big advantage are the costs: RFID transponders can be purchased very cheap, as low as 0.20 € per item.

Based on that, multiple localization algorithms were proposed in the past providing positioning results with an error as low as 0.3 m in 2D scenarios[1–3].

The available approaches only work with one person within the measurement area. But for real world appliances it is very important to calculate reasonable positioning results even when there is more than one person in a room.

In this paper we describe the existing approach in section II and its behavior in a two-person scenario in section III. Also we describe possible methods to distinguish between the users and to facilitate position estimation.

The setup and the results of a first experimental validation are shown in the fourth chapter, followed by benefits for smart environment services and our conclusions.

II. RELATED WORK

A. Passive RFID Positioning

Dealing with the problem of energy efficiency and deployment complexity we invented an approach utilizing ground mounted passive Radio Frequency Identification Tags (RFID) for device-free radio-based recognition[1], [3], [4]. This work has shown that it is possible to calculate 2D user positions with remarkable accuracy [4] and low computational complexity.

Using typical RFID hardware provides less signal processing possibilities than typically used wireless sensor nodes. For this reason our measurements regards the *Received Signal Strength Indicator* (RSSI) with can be regarded as a linear transformation of the original signal strength value.

As shown in [5] the presence of the human body does strongly affect the communication between the RFID reader hardware and the passive transponders. This can be modeled as[5]:

$$\Delta P(d_{exc}) = A d_{exc}^B \cos\left(\frac{2\pi}{\lambda} d_{exc} + \phi_{refl}\right) \qquad (1)$$

with ΔP as estimated RSSI change, wave length λ and phase shift ϕ_{refl}. The parameters A,B are subject to the multipath fading properties of the experimental environment[6]. Therefore the model needs to be re-adjusted for every new setup.

The path difference d_{exc} between the Line-of-sight (LOS) and the Non-Line-of-sight (NLOS) path is determining the relative position of a scattering user towards a specific communication link. The influence is shown in Fig. 1.
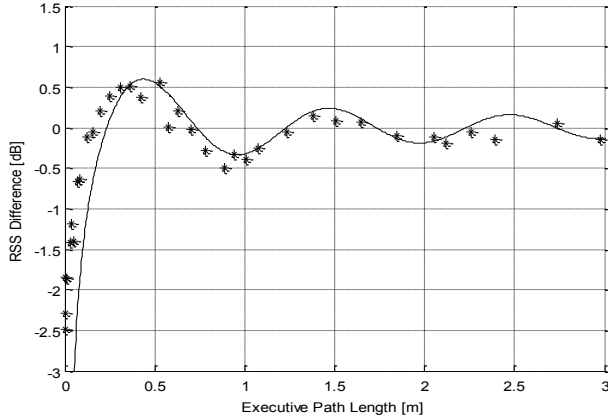
Figure 1. Theoretical model regression and experimental data points from multiple transponder scenario

Based on this model different methods for the localization of users were investigated in the past:

- Database based localization: minimizing a log-likelihood-function from the difference between an expected change of signal strength and the measurement. The results provide a maximum RMSE of 0.75 m[1].
- Geometric localization based on Linear Least Squares and Intersection Points applied on the measured signal strength differences. The results provide lower accuracy at approximately 1.61 m, while having a lower computational complexity[1].
- Training based approaches, e.g. Multi-layered Perceptrons (MLP) [5], [6]. A three layered MLP getting the RSSI differences into its input layer and providing a 2D user position out of the output layer. Evaluating different training functions and layered transfer functions it is possible to achieve accuracies as low as 0.01m MSE in a ground mounted pRFID scenario.
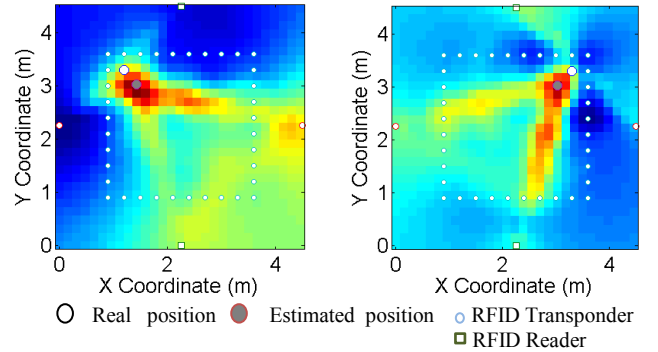
B. Passive RFID Tomography (PRT)

In our recent works [2], [4] wireless sensor network based radio tomographic imaging [7], [8] and pRFID DFL were combined. The setup consists of waist-high mounted passive transponders placed around the discretised measurement area. The RFID antennas are placed directly behind the transponder lines to guarantee a maximum power transfer.
The imaging result is calculated by using the model of Wilson et.al.[8]:

$$\Delta y = W\Delta x + n \qquad (2)$$

with Δy as matrix of RSS differences in dB, W as pre-calculated weighting matrix for every pixel-link-combination, n as zero mean gaussian noise vector and Δx as matrix of pixel attenuations.

In Figure 2 sample images of the algorithm are illustrated, the center of the maximum pixel value is regarded as the most probable user location. The algorithm can locate human with

as low as 0.3 m mean location error. In [2] we propose multiple improvements for performance and online operation.

Figure 2. Passive RFID Tomographic Images

III. METHODS

The experimental area is defined by an image vector consisting of N pixels. When a person is affecting specific links in that network (see Fig. 1), that attenuation is regarded as the sum of attenuation each pixel contributes[4].
The attenuation is measured as the received signal strength for every transponder-antenna combination. Due to the RFID protocol[7] it is difficult to set a stable power value for every transponder. Therefore a 2 phase measurement was conducted: a calibration phase with no user presence and a measurement step with scatterer in the field. The measurement vector is built by

$$\Delta y = y_{meas} - y_{cal} \qquad (3)$$

with signal strength y and RSSI difference vector Δy.
The most important part of the PRT method is the image reconstruction since the problem is ill-posed. The authors handle this by using regularization techniques. The resulting image estimation formula can be written as[8]:

$$\Delta x = (W^T W + C_x^{-1})^{-1} W^T \Delta y \qquad (4)$$

In this formula C_x denotes a covariance vector providing information about the dependence of neighboring pixels due to a zero-mean Gaussian random field [9]:

$$C_x = \sigma_x^2 e^{-d/\delta} \qquad (5)$$

with the voxel-voxel distance d and a correlation term δ determining the impact of dependence of neighboring pixels.
We have to use a weighting model only regarding the backward link between transponder and antenna because due to the experimental scenario a user can only affect this path. The forward link is regarded only as sending power supply. Regarding the model of [8] it can be described as

$$w_{ij} = \frac{1}{\sqrt{d_{t(i)\,rx(i)}}} \begin{cases} 1 & if\ d_{t(i)\,j} + d_{j\,rx(i)} < d_{t\,rx(i)} + \lambda_{backw} \\ 0 & otherwise \end{cases}$$

for the backward link, where d_{xy} is the Euclidean distance between transmitting reader antenna tx, receiving reader antenna rx and transponder t of link i. The ellipse width surrounding each link is variable by λ.
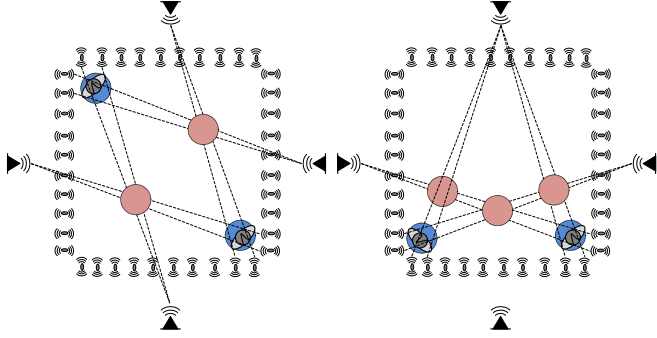

Figure 3. Influence of 2 scatterer on the field

Basic estimation for all further evaluation is the estimated pixel picture due to (4) Δx. Within one-user scenarios the maximum image pixel is used for user center estimation.
In multi-user scenarios multiple hotspots arise in the calculated picture. As you can see in Fig. 3 so called *Ghosts* can be derived, because affected links meet multiple times due to our specific geometry. There are diverse techniques required to separate the *true* positions and the *ghost* positions, some approaches are described below:

A. Maximum Removal Iteration (MRI)

High loss areas with high impact on the link measurement matrix are generally appearing where true obstacles are shadowing a higher number of communication links. Due to the geometry of our RFID setup the link density is not constant over the whole measurement field. Due to that affected links are intersecting multiple times in the field. Because the picture is calculated out of a link to pixel correlation there intersecting points also result in hot spots.
In this approach the first position estimate is the maximum pixel in the whole field. Due to the geometric properties of the link density the "ghost" result areas have a little smaller diameter and lower absolute values (cp. Fig 3).
Therefore we search for the first estimate by simply taking the center of the maximum pixel value as first position estimate:

$$E(p) = arg\max(\Delta x) \tag{7}$$

After getting that maximum all correspondent link affections needs to be removed from the measurement matrix and replaced by calibration values. Therefor we need the corresponding links i due to our weighting definition

$$i_{corr} = \forall i: (\,d_{t(i)E(p)} + d_{E(p)rx(i)} - d_{t(i)rx(i)} < \lambda_{backw}) \tag{8}$$

and replace them with the calibration value.

$$\Delta y(i_{corr}) = y_{cal} \tag{9}$$

This procedure is now being iterated until a defined picture idle variance $var_{idle}(\Delta x)$ is reached. This variance has to be calculated in every iteration step.

B. Polygon Distance Estimation (PDE)

As mentioned in [1] geometric estimation algorithms generally perform with acceptable performance but very low computational complexity.
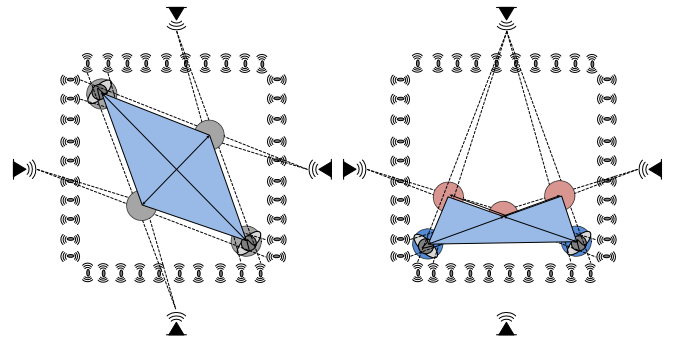The idea is to span a virtual polygon with edges on the calculated hot spots of matrix Δx (cp. Fig. 4).

Figure 4. PDE Examples

Having calculated the n_e edge points of the polygon we define the estimated user positions as intersection point with the maximum Euclidean Distance to each other:

$$E(p) = arg\max\left(\sqrt{\sum_i (n_e(1) - n_e(2))^2}\right) \tag{10}$$

Due to the field geometry, the ghost spots are always situated within the inner field belonging to the real user positions. Therefor they have a typically lower distance to each other.

C. Multi-layer Perceptron Estimation (MLPE)

In recent works[3] we show that training based approaches can perform very good, if the requirements of model based techniques are not complied sufficiently.
We try to estimate the two user positions with the help of a 3-layerd perceptron which gets the Δy data stream as its input. The hidden layer size has to be chosen due to the tradeoff between computational complexity if its larger, and degrees of freedom if its smaller. In [3] we found out that $N_h = 10$ is a good compromise.
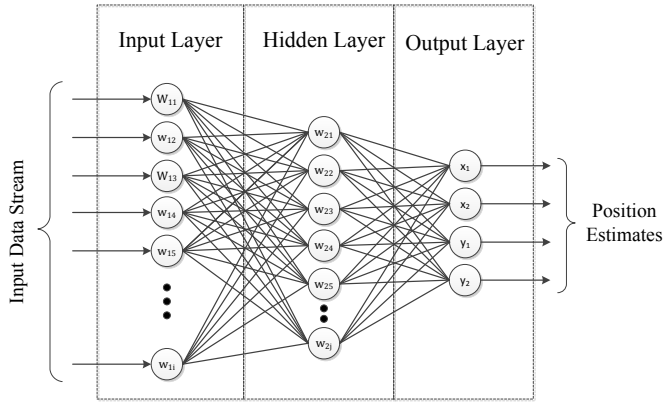
Figure 5. MLP with continuous estimation output

The neurons are calculating its output due to the following equation:

$$out = t(W \times in + B) \qquad (11)$$

with W and B as vectors of offline trained weighting and bias values. $t(x)$ is denoting a chosen transfer function which should be a combination of a logarithmic sigmoid and a linear function to get best results.
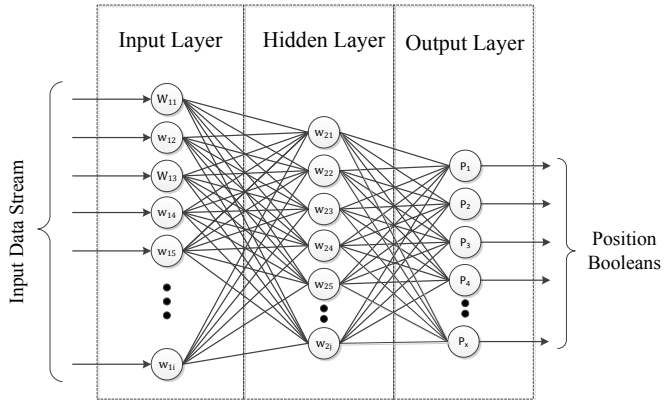

Figure 6. MLP with discrete position output

In this paper we investigate two principle Neural Network techniques: first shown in Fig. 5 the output layer provides 2 defined position coordinates. It is also possible to predefine possible user positions on the field and regard them as Boolean outputs of the perceptron (cp. Fig.6). So the output has just to be noise-filtered for getting clear true and false values.

IV. VALIDATION

A. Experimental Setup

The experimental setup is illustrated in Figure 7. It consists of three major parts: a passive UHF RFID system, a network layer and the processing workstation. We use a bistatic UHF reader from Alien Technology®[10] working in the ISM 868 MHz frequency band. For transponder powering and the backward link communication four linear polarized UHF antennas with a gain of 6 dBiL and a 70 degree azimuth beamwidth are connected to its ports. For measurements we installed a square field (edge length: 3.5m) of hip height mounted UHF transponders with a 96-bit EPC[11] compliant memory holding a unique identification number.
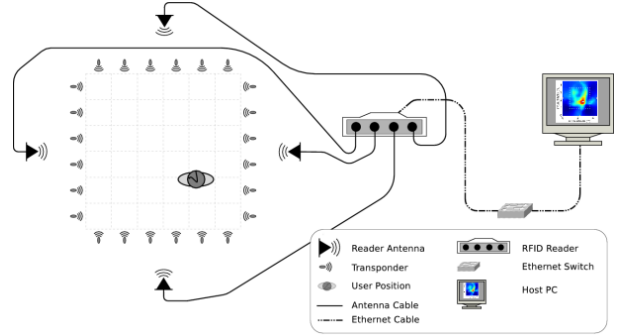

Figure 7. Experimental setup and system structure

The RFID system is connected via ethernet to the operating workstation. Every transponder answer is repeated via TCP packets to the workstation for further evaluation. The processing station is a Unix running PC with an Intel®Core™2 Quad CPU @ 4*3GHz.

The EPCglobal[11] Radio-Frequency Identity Protocol for Class-1 Generation-2 UHF RFID communication at 860-960 MHz defines baseband operations to address a smaller subset of RFID transponders. Therefore bit masking instructions are available in the readers API. Typically we have changing transponder group members due to the current position estimation. Therefore the individual 96-Bit EPC key is divided into hexadecimal subgroups used for group division.

As reference localization algorithm we used the pRFID tomography approach from Wagner et Patwari [2][4]. The evaluation script is an integrated Java/Matlab®-Script containing the RFID communication structure in Java and the evaluation code in the Matlab part.

B. Measurement Procedure

We placed 40 transponders in a square with the length of 3.1 m on the height of 0.85 m. In the middle of that square we defined 8 possible user locations. Fig. 8 shows the experimental setup. We measured 4 typical user position combinations for our 2-user scenario:

$$P = \{[1,3], [2,4], [5,7], [6,8]\}$$

In this deployment every reader antenna is powering the transponder-line in front of it. This ensures a maximum power transmission to the transponders.

The transponders are sending their data to each of the other reader antennas. Hence the operating sequence is defined as follows:

$$AS = \{[1,3],[2,4],[3,1],[4,2]\} \qquad (12)$$

with the following annotation:

[Transmitting Antenna, Receiving Antenna].

We did a calibration measurement for every transponder-AS combination with a minimum of 20 data samples to get a reliable mean signal strength value.

For the measurement phase we implemented a bitmasking algorithm, which allows us to communicate with each single transponder. Thus we defined one spin round by having data samples from every transponder. We emphasized the length of each measurement round, to get a minimum of 10 data samples per transponder-reader antenna combination.
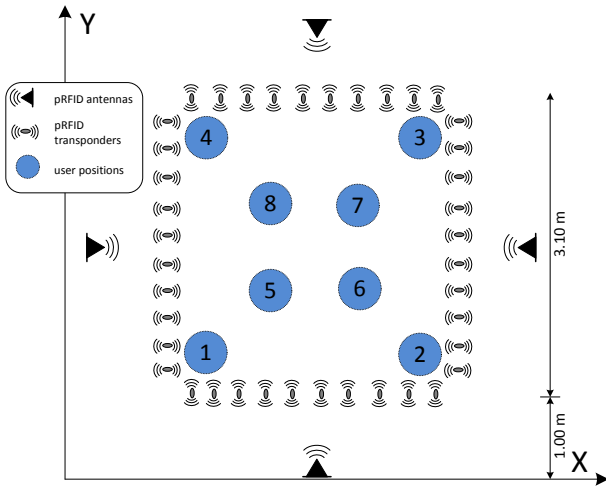

Figure 8. Experimental system structure

C. Results

Calculating the tomographic reference pictures shows the expected view with ghost hot spots within the measurement area. In Figure 9 you can see these images for 2 example measurement scenarios.

The *MRI* algorithm works hardly fine, because it has some problems with high variance pictures and ghosts with a higher diameter. The key problem is the first estimate with a detection rate of appr. 50%. The results after the first position estimate are also shown in Fig. 9.

PDE performs much better with a detection ratio of nearly 100% it reaches a much lower location error.

Approach	Mean error [m]
MRI	1.2759
PDE	0.2964
MLPE	low

Table 1. Comparison of mean location errors

The MLPE approach in its two versions is not really comparable with the other mentioned approaches. A high amount of training data leads to a detection rate of 100%. It has to be said, that this scenario can be performed very well with training based methods. The continuous version of the neural network even the binary version can estimate the original positions very accurate, but a high amount of training data is needed.
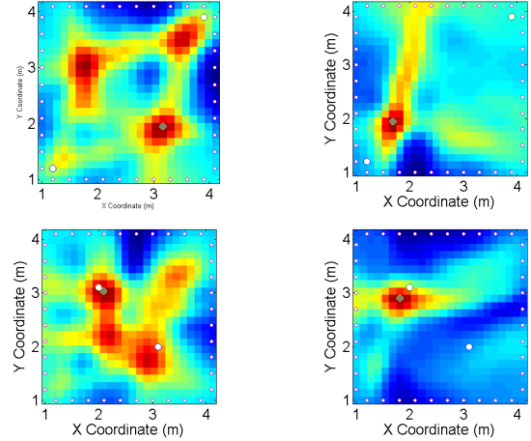

Figure 9. Reference picture (left) and MRI second phase (right) for a 2-User measurement

V. BENEFITS FOR SMART ENVIRONMENT SERVICES

Smart environmental services like ambient assisted living (AAL), i.e. for elderly care or home automation strongly rely on context information, mainly user position information. This includes static position estimates and real time tracking trajectories. Superimposed intention recognition systems rely on that data to deduce strategies for user specific assistance provision.

These environmental services, especially in an indoor environment, can benefit from user independent localization technologies, because of their non-invasive, privacy preserving structure. As already said in the introduction the RFID approach furthermore combines the advantages of easy deployment and low cost. Taking these technical advantages into account, it is possible to provide ubiquitous assistance even for older people in their familiar environment or in home environments, were complex hardware has to be invisible.

The scope of this works enhances recent feasibility studies on the field of device-free RFID localization by the possibility of multi-user recognition. This is a necessary feature, because usually there are user groups interacting in smart environments. Thus the distinction and independent tracking of multiple users is a key functionality for superimposed environmental services.

VI. CONCLUSION & FUTURE WORK

After conducting first experiments in a multi-user scenario and implementing the described approaches it has to be stated that it is possible to distinguish between 2 users and localize them with reasonable accuracy. The geometric approach performs best, but only under fixed geometric conditions. It is also possible to reach high accuracy with training based methods, but the amount of training data is very high. Possibly environmental changes on the experimental infrastructure can have a strong influence on these results.

In future a limit of users needs to be investigated, because the picture noise rises with a growing number of users in the measurement area. Another interesting point are tracking filters if the number of individuals is known.

ACKNOWLEDGMENT

REFERENCES

[1] D. Lieckfeldt, J. You, and D. Timmermann, "Exploiting RF-Scatter: Human Localization with Bistatic Passive UHF RFID-Systems," *2009 IEEE International Conference on Wireless and Mobile Computing, Networking and Communications*, no. Ic, pp. 179–184, Oct. 2009.

[2] B. Wagner, B. Striebing, and D. Timmermann, "A System for Live Localization In Smart Environments," *IEEE International Conference on Networking, Sensing and Control*, 2013.

[3] B. Wagner, D. Timmermann, G. Ruscher, and T. Kirste, "Device-free user localization utilizing artificial neural networks and passive RFID," *2012 Ubiquitous Positioning, Indoor Navigation, and Location Based Service (UPINLBS)*, pp. 1–7, Oct. 2012.

[4] B. Wagner, N. Patwari, and D. Timmermann, "Passive RFID tomographic imaging for device-free user localization," *2012 9th Workshop on Positioning, Navigation and Communication*, no. 1, pp. 120–125, Mar. 2012.

[5] D. Lieckfeldt, J. You, and D. Timmermann, "Characterizing the Influence of Human Presence on Bistatic Passive RFID-System," *2009 IEEE International Conference on Wireless and Mobile Computing, Networking and Communications*, pp. 338–343, Oct. 2009.

[6] B. Wagner and D. Timmermann, "Adaptive Clustering for Device Free User Positioning utilizing Passive RFID," *4th Workshop on Context Systems, Design and Evaluation (CoSDEO)*, 2013.

[7] Y. Kawakita, "Anti-collision performance of Gen2 Air Protocol in Random Error Communication Link," *International Symposium on Applications and the Internet Workshops (SAINTW'06)*, pp. 68–71, 2005.

[8] J. Wilson and N. Patwari, "Radio Tomographic Imaging with Wireless Networks," *IEEE Transactions on Mobile Computing*, vol. 9, no. 5, pp. 621–632, May 2010.

[9] R. K. Martin, C. Anderson, R. W. Thomas, and A. S. King, "Modelling and analysis of radio tomography," *2011 4th IEEE International Workshop on Computational Advances in Multi-Sensor Adaptive Processing (CAMSAP)*, pp. 377–380, Dec. 2011.

[10] "Alien Technology Inc." [Online]. Available: http://www.alientechnology.com/.

[11] EPCGlobal Inc., "Specification for RFID Air Interface EPC TM Radio-Frequency Identity Protocols Class-1 Generation-2 UHF RFID Protocol for Communications at 860 MHz – 960 MHz," no. October, 2008.